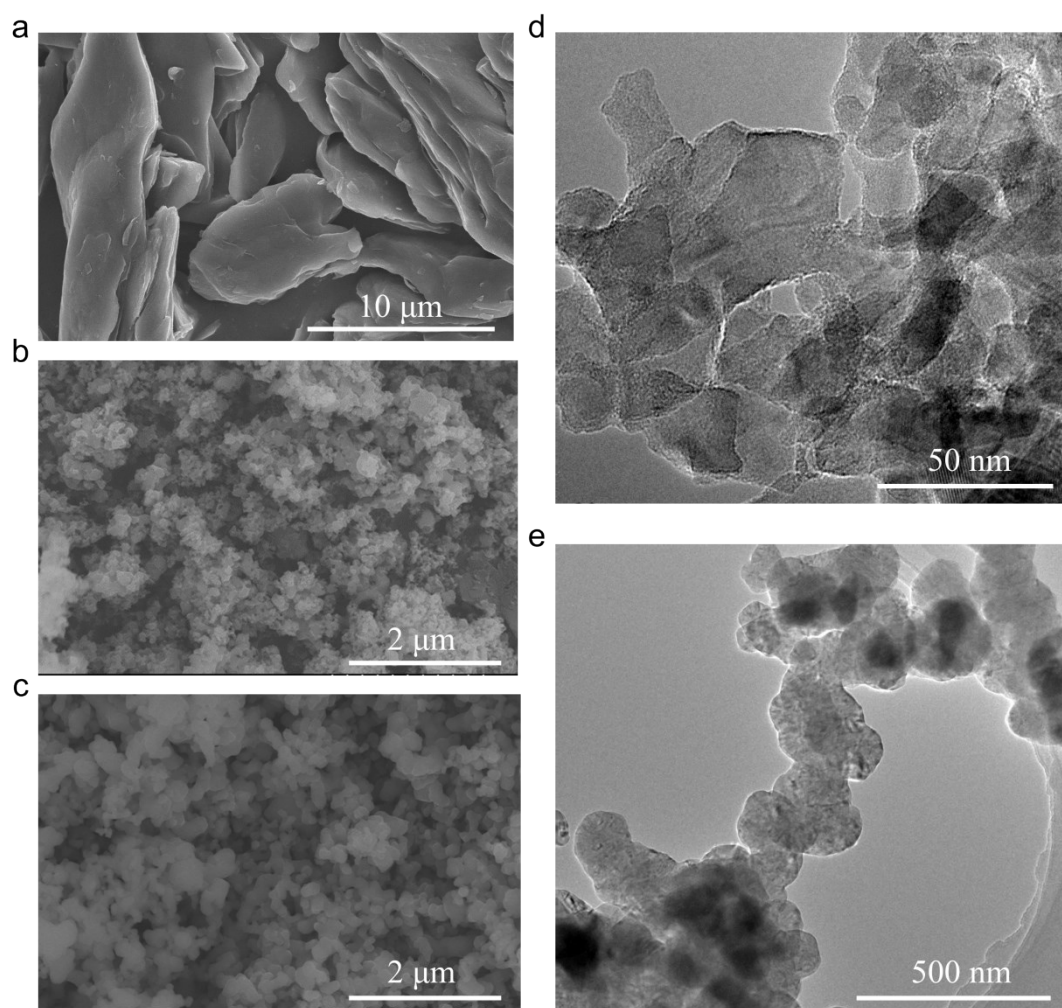


## Supporting Information

### Scalable synthesis of silicon nanoplate-decorated graphite toward advanced lithium-ion battery anodes†

Haimei Li,<sup>a,b</sup> Xianglong Li,<sup>\*b,c</sup> Denghui Wang,<sup>b,c</sup> Siyuan Zhang,<sup>b,c</sup> Wenqiang Xu,<sup>b</sup> Li-Na Zhu,<sup>\*a</sup> Linjie Zhi<sup>\*b,c</sup>

**Fig. S1-S4, Table S1, and Supplementary references**



**Fig. S1** SEM image of (a) graphite, (b) silicon nanoplates, and (c) silicon nanoparticles, as well as TEM image of (d) silicon nanoplates and (e) silicon nanoparticles.

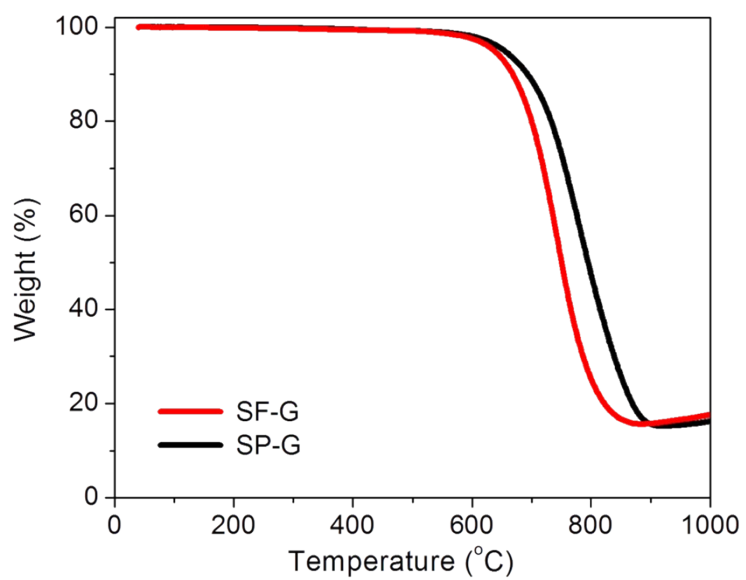


**Fig. S2** TGA curve of SF-G and SP-G.

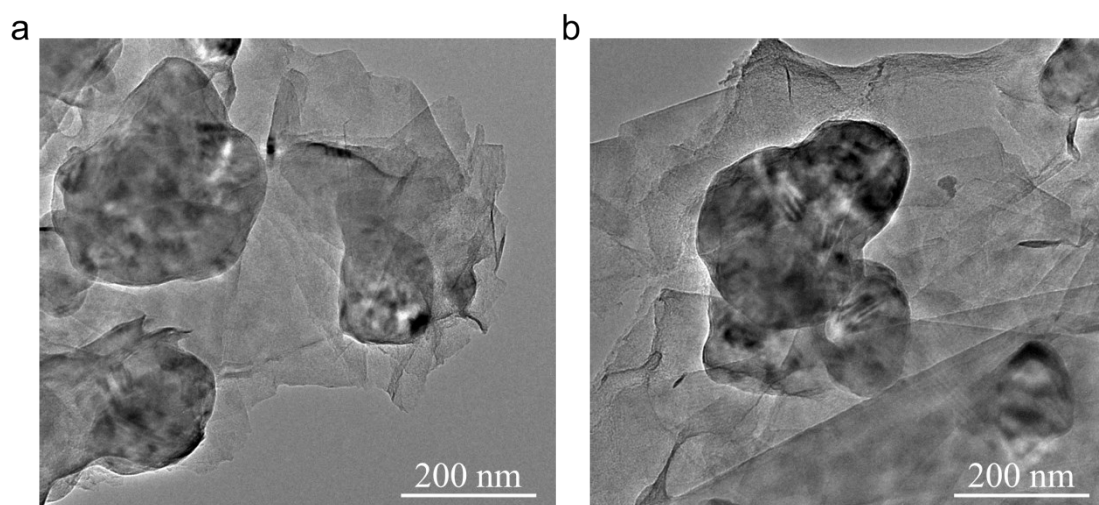


**Fig. S3** Typical TEM images of SP-G.

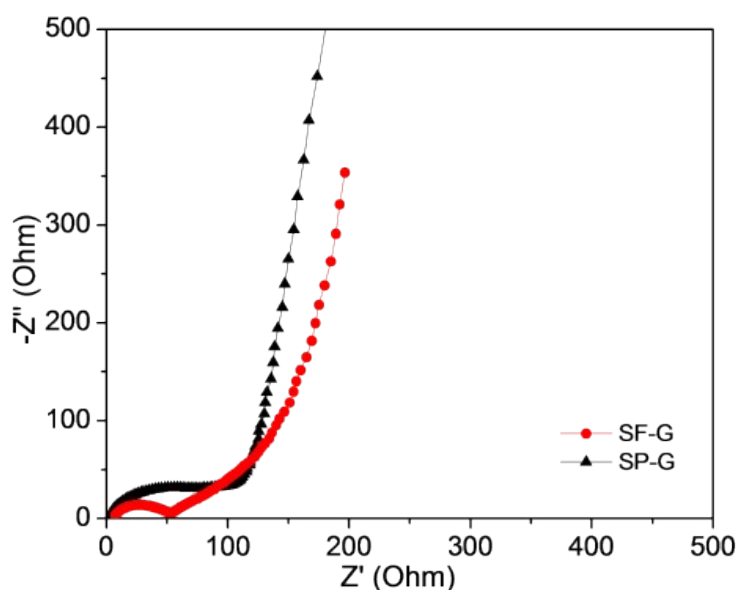


**Fig. S4** Nyquist plots obtained from EIS measurements of SF-G and SP-G. All the plots are composed of a depressed semicircle in the higher frequency region and an inclined line in the lower frequency region. The inclined line corresponds to the lithium-ion diffusion impedance, and the depressed semicircle mainly consists of the interfacial charge transfer impedance. The comparison of semicircle diameters reveals that the charge transfer resistance of SF-G is significantly smaller than that for SP-G, implying that the area-to-area contact is more competent to create fast electron transport paths between silicon and graphite. Furthermore, it should be mentioned that the Nyquist plot of SF-G shows a shorter diffusion tail in the low frequency region. This observation can be associated with the involved silicon nanoplates that facilitate the diffusion and transport of lithium ions and thus reduce the lithium ion diffusion resistance.

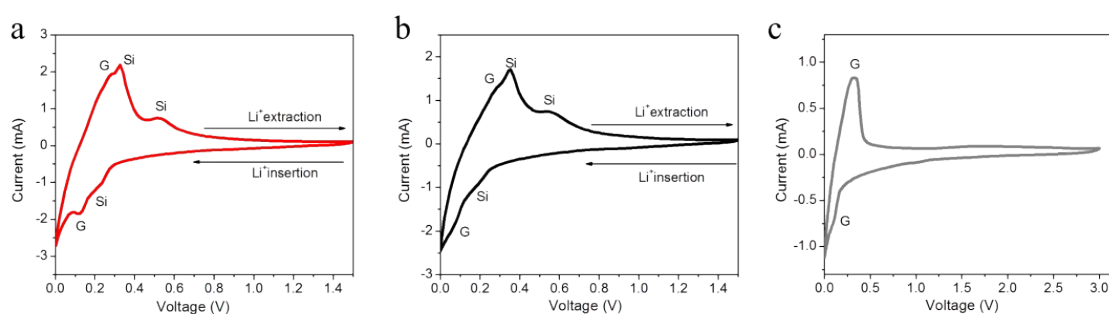


**Fig. S5** Typical CV curves of (a) SF-G, (b) SP-G, and (c) graphite.

Active material	Silicon content (wt%)	Capacity at the 1st cycle (mAh g <sup>-1</sup> )	Capacity @ the annotated cycle (mAh g <sup>-1</sup> )	Current density (mA g <sup>-1</sup> )	Capacity retention (%) /Cycles	Ref.
SF-G	~16	814	757@100th	465	93%/100 71%/500	This work
Si/Gr/C	23.3	823	763.1@100th	200	92.7/100	S1
Si/Gr/C	17	710	568@100th	130	80%/100	S2
Si/Gr/C	17.1	784	749@50th	500	95.6%/50	S3
Si/Gr/C	15.5	~750	~630@100th	500	84%/100	S4
Si/Gr/C	16	756	403@305th	200	53.3%/305	S5
Si/Gr/C	15.7	636.9	570.5@100th	0.1C	89.5%/100	S6
Si/Gr/C	9	596	~460@50th	0.5C	77%/50	S7

**Table S1** Specification and cyclic performance of SF-G and some representative silicon-graphite composites.

**Supplementary references:**

1. A. Sun, H. Zhong, X. Y. Zhou, J. J. Tang, M. Jia, F. Y. Cheng, Q. Wang, J. Yang, *Appl. Sur. Sci.*, 2019, **470**, 454–461.
2. S. Y. Kim, J. Lee, B.-H. Kim, Y.-J. Kim, K. S. Yang, M.-S. Park, *ACS Appl. Mater. Interfaces*, 2016, **8**, 12109–12117.
3. C. M. Xiao, P. He, J. G. Ren, M. Yue, Y. Y. Huang, X. Q. He, *RSC Adv.*, 2018, **8**, 27580–27586.
4. Q. Xu, J.-Y. Li, Y.-X. Yin, Y.-M. Kong, Y.-G. Guo, L.-J. Wan, *Chem. Asian J.*, 2016, **11**, 1205–1209.
5. H. Wang, J. Xie, S. C. Zhang, G. S. Cao, X. B. Zhao, *RSC Adv.*, 2016, **6**, 69882–69888.
6. J. Li, J. T. Wang, J. Y. Yang, X. L. Ma, S. G. Lu, *J. Alloys Comp.*, 2016, **688**, 1072-1079.
7. M. Ko, S. Chae, J. Ma, N. Kim, H.-W. Lee, Y. Cui, J. Cho, *Nat. Energy*, 2016, **1**, 16113.